



OPEN

Cytotoxic and chemomodulatory effects of *Phyllanthus niruri* in MCF-7 and MCF-7^{ADR} breast cancer cells

Ola E. Abdel-Sattar¹, Rasha Mosa Allam², Ahmed M. Al-Abd^{2,3}, Bharathi Avula⁴, Kumar Katragunta⁴, Ikhlas A. Khan^{4,5}, Ahmed M. El-Desoky⁶, Shanaz O. Mohamed⁷, Ali El-Halawany¹, Essam Abdel-Sattar¹  & Meselhy R. Meselhy¹

The members of the genus *Phyllanthus* have long been used in the treatment of a broad spectrum of diseases. They exhibited antiproliferative activity against various human cancer cell lines. Breast cancer is the most diagnosed cancer and a leading cause of cancer death among women. Doxorubicin (DOX) is an anticancer agent used to treat breast cancer despite its significant cardiotoxicity along with resistance development. Therefore, this study was designed to assess the potential cytotoxicity of *P. niruri* extracts (and fractions) alone and in combination with DOX against naïve (MCF-7) and doxorubicin-resistant breast cancer cell lines (MCF-7^{ADR}). The methylene chloride fraction (CH₂Cl₂) showed the most cytotoxic activity among all tested fractions. Interestingly, the CH₂Cl₂-fraction was more cytotoxic against MCF-7^{ADR} than MCF-7 at 100 µg/mL. At sub-cytotoxic concentrations, this fraction enhanced the cytotoxic effect of DOX against the both cell lines under investigation (IC₅₀ values of 0.054 µg/mL and 0.14 µg/mL vs. 0.2 µg/mL for DOX alone against MCF-7) and (1.2 µg/mL and 0.23 µg/mL vs. 9.9 µg/mL for DOX alone against MCF-7^{ADR}), respectively. Further, TLC fractionation showed that B2 subfraction in equitoxic combination with DOX exerted a powerful synergism (IC₅₀ values of 0.03 µg/mL vs. 9.9 µg/mL for DOX alone) within MCF-7^{ADR}. Untargeted metabolite profiling of the crude methanolic extract (MeOH) and CH₂Cl₂ fraction exhibiting potential cytotoxicity was conducted using liquid chromatography diode array detector-quadrupole time-of-flight mass spectrometry (LC-DAD-QTOF). Further studies are needed to separate the active compounds from the CH₂Cl₂ fraction and elucidate their mechanism(s) of action.

Several challenges for cancer treatment might result in treatment failure such as, acquired drug resistance which results in the decrease in the intracellular drug concentrations with limited cancer proliferation inhibition and ultimately metastasis¹. Accordingly, different dose regimens, higher chemotherapeutic doses or prolonged treatment might be needed to achieve similar efficacy which will lead to more adverse effects². Doxorubicin (DOX), is the standard first-line adjuvant chemotherapy in the treatment of solid tumors of disparate origins especially, early and metastatic breast cancer, one of the most common female malignant neoplasms^{3,4}. Despite showing promising clinical results, there are clinical limitations arising from its vulnerability to the development of multidrug resistance (MDR), possibly due to the overexpression of ATP binding cassette transporters as well as developing debilitating side effects hurdle against dose escalation and completion of treatment course^{5,6}. Cardiotoxicity and other multi-organ toxicities such as liver are the major limitation for doxorubicin treatment continuation and dose escalation and accordingly, result in restricted anticancer efficacy^{7,8}.

¹Pharmacognosy Department, Faculty of Pharmacy, Cairo University, Kasr El Aini St., Cairo 11562, Egypt. ²Pharmacology Department, Medical and Clinical Research Institute, National Research Centre, Dokki, Cairo 12622, Egypt. ³Biomedical Research Division, NAWAH Scientific, Mokattam, Cairo, Egypt. ⁴National Center for Natural Products Research, School of Pharmacy, University of Mississippi, University, MS 38677, USA. ⁵Division of Pharmacognosy, Department of BioMolecular Sciences, School of Pharmacy, University of Mississippi, University, MS 38677, USA. ⁶Department of Molecular Biology, Genetic Engineering and Biotechnology Research Institute (GEBRI), University of Sadat City (USC), Sadat City 32958, Egypt. ⁷School of Pharmaceutical Sciences, Universiti Sains Malaysia, 11700 Gelugor, Penang, Malaysia. ✉email: essam.abdelsattar@pharma.cu.edu.eg

Therefore, there is a necessity for a proper approach to potentiate the DOX chemotherapeutic efficacy and limit its side effects by reducing its doses. It is worth mentioning that cancer cells typically display much higher ROS levels which counteract the activity of several cytotoxic agents such as DOX⁹.

Yet, cancer cells are naturally more dependent on antioxidant systems and ROS scavenging metabolic pathways. Consequently, impairing antioxidant system may be a potential therapeutic approach against cancer¹⁰.

To this aim, natural products are gaining prominent attention in drug discovery, especially for the development of anticancer drugs. Several plant extracts and bioactive compounds demonstrated promising anticancer properties as well as chemomodulatory effects^{11,12}.

Genus *Phyllanthus* is one of the largest genus in the family Phyllanthaceae having 11 sub-genera comprising over 700 well-known species and are globally disseminated in the tropics and subtropics¹³. *Phyllanthus niruri* L. (Syn *P. amarus* Schum & Thonn) is a traditional pharmaceutical plant that has been described for its various medicinal activities such as hepatoprotective, antibacterial, antiviral, anti-diabetes, anti-obesity, antihyperlipidemic, and anti-inflammatory^{14–17}.

In recent years, *Phyllanthus* species are examples of promising sources of natural anticancer products^{18,19}. *P. niruri* demonstrated anticancer properties against lung cancer²⁰, breast cancer²¹, prostate cancer²², and hepatocellular carcinoma²³. Thanks to its antiproliferative effect on cancer cells by modulating various cell signaling pathways, reports showed its advantage of being safe on normal cells^{23,24}. Yet, its efficacy against high recurrent and resistant cancer such as breast cancer is still unclear.

In our previous work, we prepared lignan-rich extract from the aerial parts of *P. niruri* using nonconventional methods to increase the level of lignans calculated as phyllanthin²⁵. Herein, we investigated the potential cytotoxicity of the different extracts from *P. niruri* and studied the influence of their combination with DOX on the cytotoxic profile of DOX in naïve and doxorubicin-resistant breast cancer cell lines.

Materials and methods

Chemicals. Phyllanthin was purchased from Fluka (Lot # BCBL2476V, product of India). The analytical grade solvents used in the extraction and chromatographic separation were purchased from El Gomhouria for Drugs Co. (Cairo, Egypt). Precoated TLC plates (20 × 20 cm), silica gel F₂₅₄ and RP silica gel were obtained from Sigma-Aldrich chemicals (Darmstadt, Germany). Sulforhodamine-B (SRB) and doxorubicin were purchased from Sigma Chemical Co. (St. Louis, MO, USA). Acetonitrile, methanol, and formic acid used (HPLC grade) were obtained from Fisher Scientific, Waltham, MA, USA. Water was purified using a Milli-Q system (Millipore, Bedford, MA, USA).

Plant material. Samples of aerial parts of *P. niruri* L. were collected in August 2018, from Tasek Gelugor, Penang, Malaysia and the collection procedure was in compliance with the national and international guidelines and legislation. The plant materials were supplied and identified by the staff members of the Malaysian Agricultural Research and Development Institute (MARDI) through Natural Wellness Co., Cairo, Egypt. A voucher specimen (PN-01-082018B) was kept at the herbarium of the Faculty of Pharmacy, Cairo University.

Extraction and fractionation of the crude extract. The powdered aerial parts of *P. niruri* (750 g) were exhaustively extracted with MeOH (3 × 1.5 L) and another amount (100 g) was extracted with boiling distilled water (2 × 150 mL) using homogenizer (3 times each). The solvent was removed under vacuum, at a temperature not exceeding 60 °C to yield 93 g of MeOH extract (**Ext-1**) and 16 g of water extract (**Ext-2**). Part of the MeOH extract (70 g) was suspended in H₂O (600 mL) and extracted with CH₂Cl₂ (3 × 400 mL). The solvent was removed by distillation to yield CH₂Cl₂ fr. (**Fr-3**, 24.5 g). The aqueous remaining fraction (44 g) was passed through Diaion-HP20 (4 × 20 cm) and eluted with 100% water (500 mL), 50% MeOH (500 mL) followed with 100% MeOH (750 mL) to give **Fr-4** (26.2 g), **Fr-5** (13.2 g), and **Fr-6** (4.1 g), respectively. The resulting MeOH extract and CH₂Cl₂ fraction were analyzed by Liquid chromatography diode array detector-quadrupole time-of-flight mass spectrometry (LC-DAD-QTOF) and were biologically tested.

The CH₂Cl₂ fr. (10% solution in CH₂Cl₂) was subjected to preparative TLC (solvent system: n-hexane-ethyl acetate, 2:1) on silica gel plates (Silica gel 60, Merck; 0.5 mm thick, 20 × 20 cm). Each plate was divided into 4 bands (**B1–B4**) and each band was scratched, eluted with a mixture of CH₂Cl₂-MeOH (1:1), and evaporated and the the samples kept at 4 °C till use.

LC–MS analysis. *Sample preparation.* Samples from the MeOH extract and CH₂Cl₂ fraction were prepared in MeOH (LC–MS grade) in concentration of 50 mg/mL. The solution was then filtered and stored in sealed glass vials until analysis.

Liquid chromatography diode array detector-quadrupole time-of-flight mass spectrometry (LC-DAD-QToF). The liquid chromatographic system was an Agilent Series 1290 and the separation was achieved on an Acquity UPLC™ HSS C18 column (100 mm × 2.1 mm I.D., 1.8 μm). The mobile phase consisted of water with 0.1% formic acid (A) and acetonitrile with 0.1% formic acid (B) at a flow rate of 0.21 mL/min. The analysis was performed using the following gradient elution: 95% A/5% B to 35%B in 15 min, in next 5 min to 70%B and finally to 100% B in next 2 min. A 3 min wash followed each run with 100% B and an equilibration period of 5 min with 95% A/5% B. One microliter of the sample was injected. The column temperature was 40 °C.

The mass spectrometric analysis was performed with a QTOF-MS–MS (Model #G6545B, Agilent Technologies, Santa Clara, CA, USA) equipped with an ESI source using the following parameters: drying gas (N₂) flow rate, 13 L/min; drying gas temperature, 300 °C; nebulizer pressure, 30 psig, sheath gas temperature, 400 °C; sheath gas flow, 12 L/min; capillary voltage, 4000 V; nozzle voltage, 0 V; skimmer, 65 V; Oct RF V, 750 V; and

fragmentor voltage, 150 V. All the operations, acquisition and analysis of data were controlled by Agilent MassHunter Acquisition Software Ver. A.10.1 and processed with MassHunter Qualitative Analysis software Ver. B.10.00. Each sample was analyzed in positive and negative modes over the range of $m/z = 50\text{--}1100$ and extended dynamic range (flight time to m/z 1700 at 2 GHz acquisition rate). Accurate mass measurements were obtained by means of reference ion correction using reference masses at m/z 121.0509 (protonated purine) and 922.0098 [protonated hexakis (1H, 1H, 3H-tetrafluoropropoxy) phosphazine or HP-921] in positive ion mode, while at m/z 112.9856 (deprotonated trifluoroacetic acid-TFA) and 1033.9881 (TFA adducted HP-921) were used in negative ion mode. Samples were analyzed in all-ion MS-MS mode, where experiment 1 was carried out with collision energy of zero and experiment two with a fixed collision energy of 45 eV.

Cytotoxicity assay. *Cell culture.* Human breast cancer cell line (MCF-7), doxorubicin-resistant breast cancer cell line (MCF-7^{ADR}), rat normal cardiomyocytes (H9C2) and mouse normal hepatocytes (BNL) were obtained from Nawah Scientific Inc. (Mokatam, Cairo, Egypt) and cultured in DMEM (Dulbecco's modified eagle's medium), Gibco, USA. Fetal bovine serum (FBS) at a concentration of 10% and 100 units/mL of penicillin/streptomycin (PS) were added to the culture media. The cells were incubated at 37 °C in a humid environment that contained 5% CO₂.

Cell viability assay. The cell viability was determined following the method reported by Skehan et al.²⁶. MCF-7, MCF7^{ADR}, H9C2 and BNL cells were seeded in 96-well plates, approximately 10⁵/well. After treatment of DOX and/or *P. niruri* fractions and subfractions with concentrations of 0.01, 0.1, 1, 10 and 100 µg/ml for 72 h. We replaced the media with 150 µL of 10% TCA (trichloroacetic acid) (Merck) for 1 h at 4 °C, followed by 5 times washing with distilled water. After that, we added 70 µL of 0.4% w/v SRB solution (Sigma-Aldrich) at room temperature for ten minutes in the dark. Cells were washed with 1% acetic acid (Merck) 3 times and allowed to a 24 h air-dry. Then, we added 150 µL of Tris Base (10 mM) (Merck) and the O.D. was determined at 540 nm by a microplate reader (FluoStar Omega, BMG Labtec, Ortenberg, Germany).

Measurement of intracellular GSH Level. MCF-7^{ADR} cells were treated with DOX and B2 alone or combined at their pre-determined IC₅₀ values for 48 h. After treatment, cells were washed with PBS, trypsinized, centrifuged, and pellets were lysed using 0.5 ml of ice-cold lysis buffer (Cat No: FNN001; Invitrogen). The intracellular GSH levels were determined using the commercially available colorimetric kit to determine the GSH content (Biodiagnostics Company, Cairo, Egypt) according to the manufacturer's instructions²⁷. The total protein content in the cell lysate was determined using Bradford method for normalization.

Data analysis. The dose–response curves of compounds were investigated applying the E_{max} model as previously described²⁸. The combination index (CI) was calculated as previously described²⁹. Drug interactions are classified as additive if CI is between 0.8 and 1.2, antagonistic if CI is > 1.2, and synergistic if CI is < 0.8. All data are presented as means ± SD (n = 3). Analysis of variance (ANOVA) with Tukey's post-hoc test ($P < 0.05$) was applied using GraphPad Prism Software version 6.

Results

RP-LC-DAD-ESI-QTOF-MS profiling of methanol extract and methylene chloride fraction. The metabolite profiling of the methanol extract (MeOH) and the methylene chloride fraction (CH₂Cl₂) with potential cytotoxicity was analysed using liquid chromatography diode array detector-quadrupole time-of-flight mass spectrometry (LC-DAD-QToF). Figures 1 and 2 showed the base peak chromatograms (BPC) of the MeOH and the active CH₂Cl₂ fraction in negative and positive modes. Adopted analytical setup in both ESI modes led to the identification of 53 in both extracts with low abundance of metabolites 5, 9–14, within 30 min (Table 1). The metabolites were tentatively characterized based on their UV spectra (254, 280 and 330 nm), retention time, accurate mass, and MS fragmentation patterns and by comparing their mass spectra with those reported in the phytochemical dictionary of natural products database (CRC) and from the reported literature^{30–33}.

The identified compounds are represented by 42 phenolic acids and phenolic derivatives, 7 fatty acids, an amino acid, a sugar derivative, an alkaloid, and a dicarboxylic (Fig. 3 and Table 1). Most of peaks belonging to acids and phenolics were observed in negative ion mode (Table 1) showing [M–H][−] ions with the loss of one mass unit, except for compound 5 which was observed in positive mode. Details of metabolites assignment will be discussed in the coming section.

Biological screening. *Cytotoxicity assessment of P. niruri.* Sulforhodamine B (SRB) assay was used to assess the potential cytotoxicity of six extracts of *P. niruri*, including total methanol (Ext-1), aqueous (Ext-2), CH₂Cl₂ (Fr-3), and diaion fractions (Fr-4: water, Fr-5: 50% MeOH and Fr-6: 100% MeOH), against naïve breast cancer cell line (MCF-7) and doxorubicin-resistant breast cancer cell line (MCF-7^{ADR}).

All the tested fractions except for Fr-3 did not show good cytotoxicity against the two cell lines since their IC₅₀ values were higher than 100 µg/mL (Table 2). On the other hand, Fr-3 showed substantial cytotoxicity against MCF-7 and MCF-7^{ADR} cells with IC₅₀ values of 97.2 ± 1.13 µg/mL and 51.1 ± 0.93 µg/mL, respectively. Interestingly, MCF-7^{ADR} cells (Dox-resistant) were more sensitive than MCF-7 cells (Naïve) to Fr-3 treatment (Table 2).

Chemomodulatory effect of P. niruri to doxorubicin (DOX) within naïve and resistant breast cancer cells. To study the outcome of *P. niruri* on the cytotoxic profile of DOX in MCF-7 and MCF-7^{ADR} cells, we assessed the

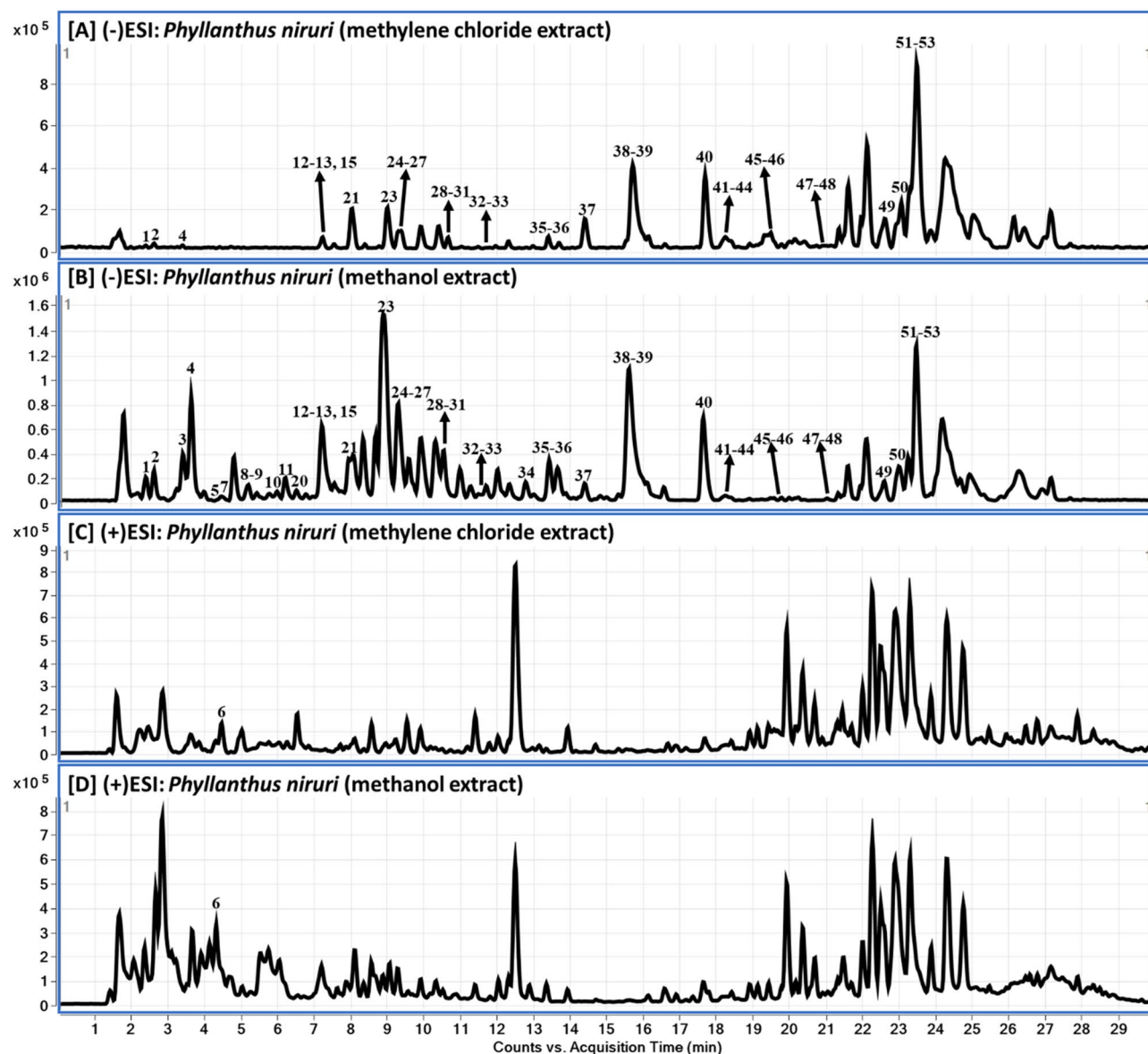


Figure 1. LC-QToF total Ion Chromatograms (TOC) of the CH_2Cl_2 and MeOH extract of *P. niruri*: in negative (A, B) and positive modes and (C, D).

dose–response curves of DOX alone and in combination with the different extracts of *P. niruri* (Fig. 1S-A, B) (Table 3).

The chemomodulatory effect of *P. niruri* extracts and fractions at noncytotoxic concentrations were studied along with serial concentrations of DOX within breast cancer cells using SRB assay as described in the previous section.

In MCF-7 cells, DOX exerted a dose-dependent cytotoxic activity, and the viability started to decrease markedly at a concentration of 0.1 $\mu\text{g}/\text{mL}$ with an IC_{50} value of $0.2 \pm 0.06 \mu\text{g}/\text{mL}$ (Fig. 1S-A). Except for Fr-3, all tested extracts, and fractions of *P. niruri* (Ext-1, Ext-2, Fr-4, Fr-5, and Fr-6) at a sub-toxic concentration (100 $\mu\text{g}/\text{mL}$) in combination with DOX did not improve the cytotoxic/antiproliferative effect of DOX against MCF-7 cells. This can be observed from the increase of IC_{50} values of DOX to ~ 10 times after combination with the different extracts. Conversely, the combination of DOX with a sub-cytotoxic concentration of Fr-3 (10 $\mu\text{g}/\text{mL}$), significantly increased the antiproliferative/cytotoxic effect of DOX against MCF-7 cells; the IC_{50} values of DOX were $0.2 \pm 0.06 \mu\text{g}/\text{mL}$ and 0.054 ± 0.001 alone and in combination with Fr-3, respectively (Fig. 1S-A). A similar result was observed for the combination of DOX with Fr-3 at higher concentration (100 $\mu\text{g}/\text{mL}$) and IC_{50} value were decreased to $0.014 \pm 0.002 \mu\text{g}/\text{mL}$ (1S-A).

Similarly, in MCF-7^{ADR} cells, DOX also showed gradient cytotoxic activity with increasing concentration; viability started to drop significantly at a concentration of 1 $\mu\text{g}/\text{mL}$ with an IC_{50} value of $9.9 \pm 1.1 \mu\text{g}/\text{mL}$ (Fig. 1S-B). Unlike the MCF-7 cell line, combining Ext-1, Fr-5, and Fr-6 with DOX significantly improved the cytotoxic profile of DOX in MCF-7^{ADR} cells, decreasing both the resistant fraction and IC_{50} of DOX to $0.27 \pm 0.01 \mu\text{g}/\text{mL}$, $1.9 \pm 0.45 \mu\text{g}/\text{mL}$ and $3.3 \pm 0.07 \mu\text{g}/\text{mL}$, respectively. Additionally, a more improvement in the cytotoxic profile

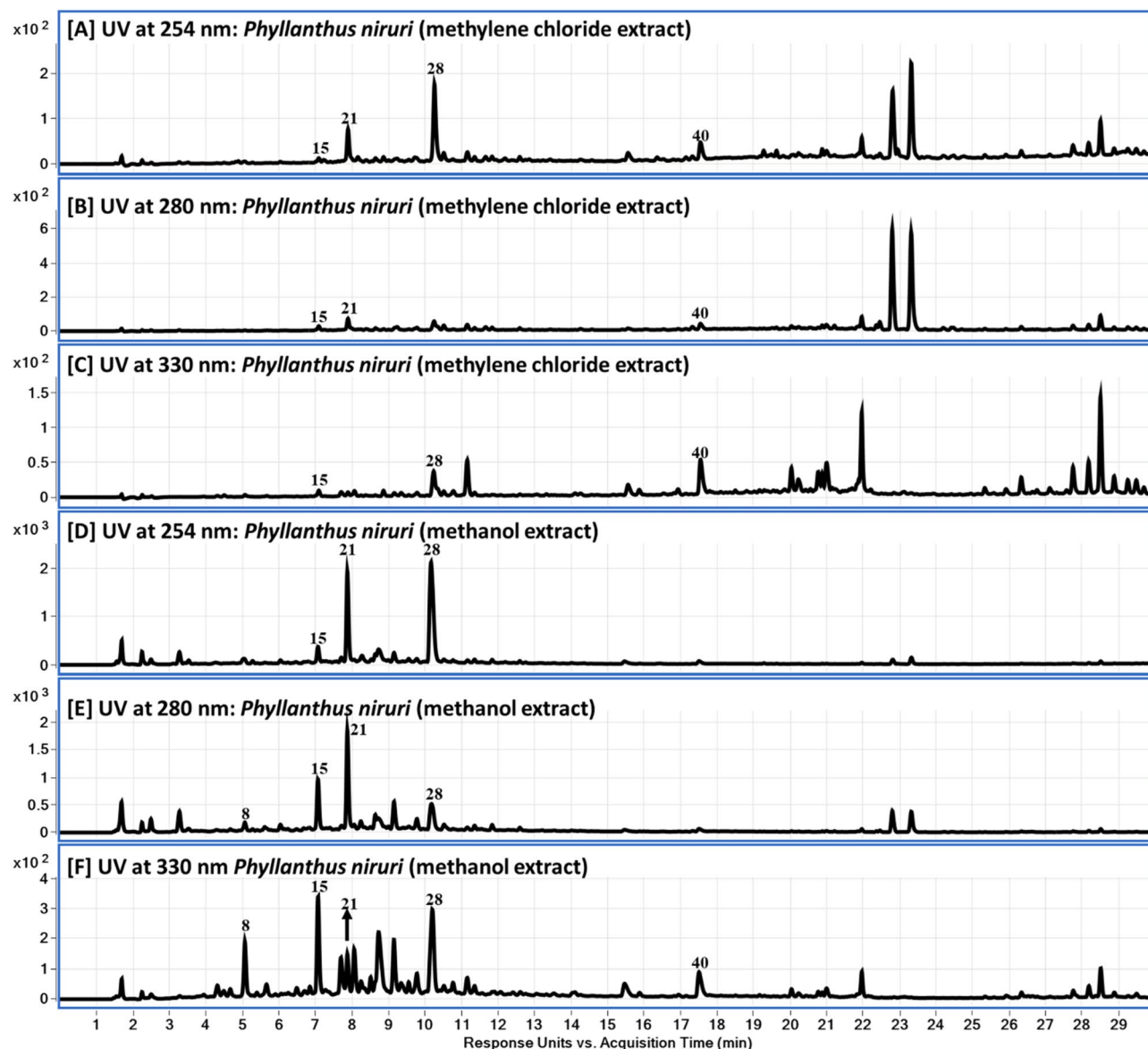


Figure 2. LC-DAD chromatograms of the CH_2Cl_2 fraction (A–C) and MeOH extract (D–F) of *P. niruri*. at 254, 280 and 330 nm.

of DOX was observed after the combination with **Fr-3** (10 $\mu\text{g}/\text{mL}$), decreasing IC_{50} of DOX to $0.23 \pm 0.01 \mu\text{g}/\text{mL}$ along with abolishing the resistant fraction. On the other hand, the combination of **Fr-4** with DOX did not significantly influence the cytotoxic/antiproliferative activity of DOX against MCF-7^{ADR} cells.

The results of these two cell lines can declare that **Fr-3** possessed the most promising chemomodulatory effect for DOX in breast cancer cells. Therefore, additional subfractions from **Fr-3** were prepared and assessed for further cytotoxic and chemomodulatory potential.

Cytotoxicity and chemomodulatory assessment of different subfractions (B1–B4) of Fr-3 on MCF-7 and MCF-7^{ADR} cells. Four TLC subfractions from **fr-3** (CH_2Cl_2) were obtained by preparative TLC and named **B1**, **B2**, **B3**, and **B4**. In MCF-7 cells, all the tested subfractions didn't show observable cell-killing effects even until 100 $\mu\text{g}/\text{mL}$ concentration. Conversely, in MCF-7^{ADR} cells, all subfractions showed cell-killing effects at a concentration of 100 $\mu\text{g}/\text{mL}$ with calculated IC_{50} values of $188.6 \pm 2.3 \mu\text{g}/\text{mL}$, $86.4 \pm 1.5 \mu\text{g}/\text{mL}$, $100.4 \pm 1.8 \mu\text{g}/\text{mL}$ and $112.7 \pm 2 \mu\text{g}/\text{mL}$ for **B1**, **B2**, **B3** and **B4** respectively (Table 4). It is worth mentioning that MCF-7^{ADR} cells were more sensitive to treatment with these subfractions. Accordingly, it was selected to further investigate the chemomodulatory effect of these subfractions on DOX. Combinations of the four subfractions (**B1–4**) with DOX were clearly synergistic with very low CI-values of 0.157, 0.003, 0.038, 0.061, respectively (Table 5). Based on these CI-values, **B2** was the most promising fraction that significantly reduced the IC_{50} of DOX from 9.9 ± 1.1 to 0.03 ± 0.001 and abolished the resistance fraction from 5.2 ± 0.04 to nearly zero (Table 5). It merits mentioning that subfractions combinations with DOX drastically improved the cytotoxic profile of DOX against MCF-7^{ADR} (Fig. 2S).

#	RT (min)	Compound Name	CH ₂ Cl ₂	MeOH	Chemical class	Molecular Formula	Exact mass	[M + H] ⁺	Fragment ions	[M-H] ⁻	Fragment ions
1	2.4	2-Deoxy-2,3-dehydro- <i>N</i> -acetylneuraminic acid	√	√	Alpha-keto acid sugars	C ₁₁ H ₁₇ NO ₈	291.0954	-	-	290.0882 (290.0881) ⁺	200.0567 [M-H-C ₃ H ₆ O ₃] ⁻ , 128.0356 [M-H-C ₃ H ₆ O ₃ -C ₃ H ₄ O ₂] ⁻
2	2.6	β-glucogallin 1- <i>O</i> -galloyl-β-D-glucopyranose,	√	√	Phenolic acid glycoside	C ₁₃ H ₁₆ O ₁₀	332.0743	-	-	331.0678 (331.0671)	211.0246 [M-H-C ₄ H ₈ O ₄] ⁻ , 169.0143 [M-H-C ₆ H ₁₀ O ₅] ⁻ , 125.0244 [M-H-C ₆ H ₁₀ O ₅ -CO ₂] ⁻
3	3.4	Gallic acid	√	√	Phenolic acid	C ₇ H ₆ O ₅	170.0215	171.0289 (171.0288)	-	169.0146 (169.0142)	125.0245 [M-H-CO ₂] ⁻ , 107.0139 [M-H-CO ₂ -H ₂ O] ⁻
4	3.6	Vanillic acid 4-sulfate	√	√	Phenolic acid	C ₈ H ₈ O ₇ S	247.9991	-	-	246.9922 (246.9918)	203.0019 [M-H-CO ₂] ⁻ , 121.0296 [M-H-CO ₂ -SH ₂ O] ⁻ , 108.0220 [M-H-CO ₂ -SH ₂ O ₃ -CH] ⁻ , 96.9604 [H ₂ SO ₄] ⁻ , 80.9656 [H ₂ SO ₃] ⁻
5	4.07	Sesbanimide A	√*	√	Polyketide alkaloid	C ₁₅ H ₂₁ NO ₇	327.1318	328.1399 (328.1391)	310.1290 [M + H-H ₂ O] ⁺ , 250.1655 [M + H-H ₂ O-C ₂ H ₄ O ₂] ⁺ , 232.1550 [M + H-2H ₂ O-C ₂ H ₄ O ₂] ⁺ , 132.0811 [M + H-2H ₂ O-C ₂ H ₄ O ₂ -C ₄ H ₄ O ₃] ⁺ , 120.0810 [M + H-2H ₂ O-C ₂ H ₄ O ₂ -C ₅ H ₄ O ₃] ⁺	326.1243 (326.1245)	-
6	4.30	Phenylalanine	√	√	Amino acid	C ₉ H ₁₁ NO ₂	165.0790	166.0855 (166.0863)	120.0479	164.0719 (164.0717)	-
7	4.44	Caffeoylglucaric acid	√	√	Phenolic acid	C ₁₅ H ₁₆ O ₁₁	372.0693	-	-	371.0619 (371.0620)	315.0720 [M-H-C ₂ O ₂] ⁻ , 209.0306 [M-H-C ₂ O ₂ -C ₇ H ₆ O] ⁻
8	5.2	Dihydrocaffeic acid 3- <i>O</i> -glucuronide	√	√	Phenolic acid glycoside	C ₁₅ H ₁₈ O ₁₀	358.0900	-	-	357.0826 (357.0827)	269.0336, 219.0512, 151.0402, 123.0451
9	5.3	Protocatechuic acid	√*	√	Phenolic acid	C ₇ H ₆ O ₄	154.0266	-	-	153.0194 (153.0193)	-
10	5.75	Dihydro virganin	√*	√	phenolic	C ₂₆ H ₂₄ O ₁₈	624.0963	-	-	623.0883 (623.0890)	355.0665 [M-H-C ₆ H ₈ O ₈] ⁻ , 234.0405 [M-H-C ₉ H ₈ O ₈ -C ₇ H ₅ O ₂] ⁻
11	6.3	1,6-Digalloylglucose; D-pyranose-form	√*	√	Phenolic glycoside	C ₂₀ H ₂₀ O ₁₄	484.0853	-	-	483.0776 (483.0780)	169.0141, 125.0246
12	7.1	Phyllanthusiin B/ Phyllanthusiin G/ Phyllanemblinin C	√*	√	ellagitannins	C ₄₁ H ₃₀ O ₂₈	970.0924	-	-	969.0850 (969.0851)	925.0955
13	7.7										
14	9.1										

Continued

#	RT (min)	Compound Name	CH ₂ Cl ₂	MeOH	Chemical class	Molecular Formula	Exact mass	[M + H] ⁺	Fragment ions	[M-H] ⁻	Fragment ions
15	7.2	Brevifolin carboxylic acid	√	√	Phenol carboxylic acid	C ₁₃ H ₈ O ₈	292.0219	-	-	291.0157 (291.0146)	247.0250 [M-H-CO ₂] ⁻ , 219.0294 [M-H-CO ₂ -CO] ⁻ , 191.0344 [M-H-CO ₂ -2CO] ⁻ , 145.0292, 119.0505
16	7.56	Methyl gallate	√	√	Phenolic acid ester	C ₈ H ₈ O ₅	184.0372	-	-	183.0298 (183.0299)	124.0167 [M-H-CH ₃ -CO ₂] ⁻
17	7.8	Geraniin /Phyllanthusiin A/Geraniinic acid B	√	√	ellagitannin	C ₄₁ H ₂₈ O ₂₇	952.0818	-	-	951.0740 (951.0745)	-
18	9.8										
19	12.2										
20	6.9	Corilagin/1-O-Galloyl-6-O-luteoyl-α-D-glucopyranose	√	√	ellagitannins glycoside	C ₂₇ H ₂₂ O ₁₈	634.0806	652.1146 (652.1144) [M + NH ₄] ⁺	465.0666 [M + H-C ₇ H ₆ O ₅] ⁺	633.0743 (633.0733)	463.0517 [M-H-C ₆ H ₆ O ₅] ⁻ , 300.9995, 275.0202
21	8.1										
22	8.8	Phyllanthusiin C	√	√	ellagitannin	C ₄₀ H ₃₀ O ₂₆	926.1025	-	-	925.0950 (925.0953)	511.0559
23	8.84	3,5,7-Trihydroxyflavone-8-sulfonic acid; 3-O-β-D-Glucopyranoside (Galangin-8-sulfonic acid, glucopyranoside)	√	√	Flavonoid = flavone	C ₂₁ H ₂₀ O ₁₃ S	512.0625	-	-	511.0555 (511.0552)	349.0026 [M-H-C ₆ H ₁₀ O ₅] ⁻ , 319.9996 [M-H-C ₆ H ₁₀ O ₅ -CHO] ⁻ , 290.9974 [M-H-C ₆ H ₁₀ O ₅ -2CHO] ⁻ , 269.0457 (galangin)
24	9.29	Brevifolin	√	√	Phenolic	C ₁₂ H ₈ O ₆	248.0015	-	-	247.0252 (247.0248)	219.0295, 191.0345, 145.0290, 117.0342
25	9.5	Phyllanemblinin A	√	√	Ellagitannins	C ₂₇ H ₂₀ O ₁₇	616.0700	-	-	615.0622 (615.0628)	300.9994, 169.0145
26	9.7	Quercetin-xylosylglucoside	√	√	Flavonoid = flavonol	C ₂₆ H ₂₈ O ₁₆	596.1377	597.1454 (597.1450)	303.0493	595.1299 (595.1305)	300.0272
27	9.90	Methylbrevifolin carboxylate	√	√	Phenolic	C ₁₄ H ₁₀ O ₈	306.0376	307.0453 (307.0448)	183.0921	305.0306 (305.0303)	273.0043 [M-H-CH ₃ OH] ⁻ , 245.0085 [M-H-CH ₃ OH-CO] ⁻ , 217.0136 [M-H-CH ₃ OH-2CO] ⁻ , 201.0186 [M-H-CH ₃ OH-CO-CO ₂] ⁻ , 189.0189 [M-H-CH ₃ OH-3CO] ⁻ , 173.0237 [M-H-CH ₃ OH-2CO-CO ₂] ⁻ ,
28	10.30	Ellagic acid	√	√	Phenolic acid	C ₁₄ H ₆ O ₈	302.0063	-	-	300.9999 (00.9990)	283.9958 [M-H-OH] ⁻ , 257.0072 [M-H-CO ₂] ⁻ ,
29	10.35	Quercetin-3-O-rutinoside	√	√	Flavonoid = flavonol	C ₂₇ H ₃₀ O ₁₆	610.1534	611.1611 (611.1607)	303.0501	609.1462 (609.1461)	301.0351
30	10.6	4-O-Brevifolin-carbonyl-1-O-galloyl-3,6-O-hexahydroxydiphenyl-D-glucopyranose	√	√	Phenolic	C ₄₀ H ₂₈ O ₂₅	908.0920			907.0847 (907.0844)	611.0708, 169.0141

Continued

#	RT (min)	Compound Name	CH ₂ Cl ₂	MeOH	Chemical class	Molecular Formula	Exact mass	[M + H] ⁺	Fragment ions	[M-H] ⁻	Fragment ions
31	10.88	Quercetin- <i>O</i> -hexoside	√	√	Flavonoid = flavonol	C ₂₁ H ₂₀ O ₁₂	464.0955	-	-	463.0877 (463.0877)	300.0257 [M-H-Hex] ⁻ , 271.0252 [M-Hex-CH ₂ O] ⁻ , 255.0299 [M-Hex-CO-H ₂ O] ⁻ , 151.0036
32	11.5	kaempferol 3- <i>O</i> -rutinoside	√	√	Flavonoid = flavonol	C ₂₇ H ₃₀ O ₁₅	594.1585	595.1661 (595.1657)	287.0556	593.1520 (593.1512)	285.0413
33	11.96	Chebulinic acid	√	√	Ellagitannins	C ₄₁ H ₃₂ O ₂₇	956.1131	-	-	955.1048 (955.1058)	923.0789 [M-H-CH ₄ O] ⁻ , 879.0899 [M-H-CH ₄ O-CO ₂] ⁻ , 611.0708 [M-H-CH ₄ O-CO ₂ -C ₁₁ H ₈ O ₈] ⁻ , 351.0176 [M-H-CH ₄ O-CO ₂ -C ₁₁ H ₈ O ₈ -C ₁₀ H ₁₂ O ₈] ⁻ , 300.9988 [ellagic acid] ⁻
34	12.72	Phyllanthusiin U	√	√	Ellagitannins	C ₄₀ H ₂₈ O ₂₆	924.0869	-	-	923.0792 (923.0796)	461.0359, 300.9988 [ellagic acid]
35	13.4	Azelaic acid	√	√	Dicarboxylic acid	C ₉ H ₁₆ O ₄	188.1049	-	-	187.0974 (187.0976)	-
36	13.7	3,4,5,7-Tetrahydroxyflavone-8-sulfonic acid	√	√	Flavonoid = flavone	C ₁₅ H ₁₀ O ₉ S	366.0046	-	-	364.9973 (364.9973)	285.0403 [M-H-SO ₃] ⁻
37	14.43	4-Hydroxybenzoic acid	√	√	Phenolic acid	C ₇ H ₆ O ₃	138.0317	-	-	137.0245 (137.0244)	93.0350 [M-H-CO ₂] ⁻ , 75.0243 [M-H-CO ₂ -H ₂ O] ⁻
38	15.65	3,5,7-Trihydroxyflavone-8-sulfonic acid (Galangin-8-sulfonic acid)	√	√	Flavonoid = flavone	C ₁₅ H ₁₀ O ₉ S	350.0096	-	-	349.0032 (349.0024)	269.0456 (galangin)
39	15.97		√	√							
40	17.7	Niruriflavone	√	√	Flavonoid = flavone	C ₁₆ H ₁₂ O ₈ S	364.0253	-	-	363.0187 (363.0180)	347.9944, 268.0376, 151.0035
41	18.21	Trihydroxy-octadecadienoic acid	√	√	Fatty acid	C ₁₈ H ₃₂ O ₅	328.2250	-	-	327.2175 (327.2177)	285.0797, 215.1289, 171.1027, 85.0299
42	18.40		√	√							
43	18.60		√	√							
44	18.90	Trihydroxy-octadecanoic acid	√	√	Fatty acid	C ₁₈ H ₃₄ O ₅	330.2406	-	-	329.2332 (329.2333)	
45	19.75		√	√							
46	19.98		√	√							
47	21.0		√	√							
48	21.4	Nirtetralin	√	√	Lignan	C ₂₄ H ₃₀ O ₇	430.1992	431.2054 (431.2064)	-	-	-
49	22.7	Phyltetralin	√	√	Lignan	C ₂₄ H ₃₂ O ₆	416.2199	417.2278 (417.2272)	151.0755	-	-
50	22.9	Phyllanthin	√	√	Lignan	C ₂₄ H ₃₄ O ₆	418.2355	419.2428 436.2694 (436.2691) 441.2248 (441.2249)	184.0740, 151.0764	-	-
51	23.4	Hypophyllanthin	√	√	Lignan	C ₂₄ H ₃₀ O ₇	430.1992	431.2065 (431.2064)	-	-	-
52	23.5	Niranthin	√	√	Lignan	C ₂₄ H ₃₂ O ₇	432.2148	433.2221 455.2045 (455.2040)	-	-	-
53	23.6	Isolintetralin	√	√	Lignan	C ₂₃ H ₂₈ O ₆	400.1886	401.1961 (401.1958)	151.0751	-	-

Table 1. Tentative identification and characterization of phytochemical compounds in *Phyllanthus niruri* leaf and stem using LC-QToF in positive and negative ionization modes. Significant values are in bold. *Theoretical accurate mass; Compound #5, 9–14 are present in low abundances in methylene chloride extracts.

Safety assessment of B2-fraction on H9C2 and BNL cells. The most promising cytotoxic fraction (B2) was further assessed for its possible cardiotoxic and/or hepatotoxic effects. H9C2 (normal cardiomyocyte) and BNL

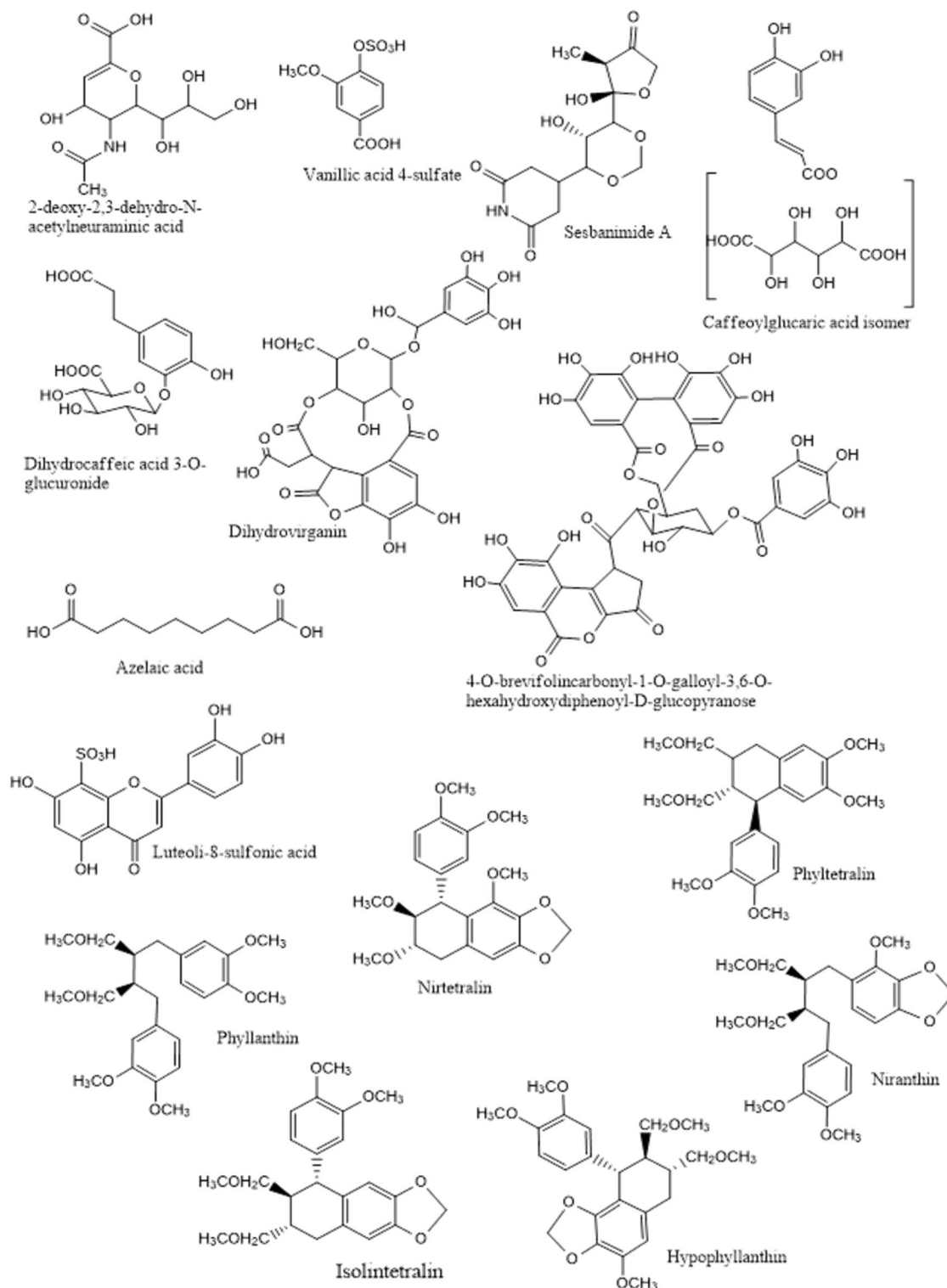


Figure 3. Examples of structure of some compound identified in *P. nirri*.

(normal hepatocytes) were incubated with B2 for 72 h, and cell viability was assessed by SRB and compared with the cell viability of DOX (Fig. 3S).

Dox inhibited cell proliferation of both H9C2 and BNL cells in a dose-dependent manner, with IC_{50} values of $0.0153 \pm 0.001 \mu\text{g/ml}$ and $0.0571 \pm 0.002 \mu\text{g/ml}$, respectively. While B2-fraction did not affect the cell viability of both H9C2 and BNL cells up to a concentration of $100 \mu\text{g/ml}$, indicating the safety of B2 fraction on heart and liver normal cells in contrast to DOX (Fig. 3S).

Extract or fraction	MCF-7		MCF-7 ^{ADR}	
	IC ₅₀ (µg/mL)	R-fraction (%)	IC ₅₀ (µg/mL)	R-fraction (%)
Ext-1	> 100	N/A	> 100	N/A
Ext-2	> 100	N/A	> 100	N/A
Fr-3	97.2 ± 1.13	N/A	51.1 ± 0.93	15.8 ± 0.7
Fr-4	> 100	N/A	> 100	N/A
Fr-5	> 100	N/A	> 100	N/A
Fr-6	> 100	N/A	> 100	N/A

Table 2. Cytotoxic activity of *P. niruri* of various extracts and fractions against MCF-7 and MCF-7^{ADR} cell lines. #N/A means not applicable.

Extract or fraction	MCF-7		MCF-7 ^{ADR}	
	(IC ₅₀ µg/mL)	R-fraction (%)	(IC ₅₀ µg/mL)	R-fraction (%)
DOX	0.2 ± 0.06	0.44 ± 0.03	9.9 ± 1.1	5.2 ± 0.04
DOX + Ext-1 (100 µg/mL)	1.2 ± 0.08*	1.7 ± 0.3	0.27 ± 0.01*	N/A
DOX + Ext-2 (100 µg/mL)	1.9 ± 0.12*	N/A	38 ± 2.3*	N/A
DOX + Fr-3 (10 µg/mL)	0.054 ± 0.001*	N/A	0.23 ± 0.01*	N/A
DOX + Fr-4 (100 µg/mL)	1.6 ± 0.13*	N/A	9.9 ± 0.82	N/A
DOX + Fr-5 (100 µg/mL)	1.2 ± 0.1*	N/A	1.9 ± 0.45*	0.73 ± 0.01
DOX + Fr-6 (100 µg/mL)	0.8 ± 0.02*	1.9 ± 0.08	3.3 ± 0.07*	N/A

Table 3. Chemomodulatory effects of *P. niruri* extracts and fractions on the cytotoxicity of DOX against MCF-7 and MCF-7^{ADR} cell lines. #N/A means not applicable. Data are presented as mean ± SD; n = 3. *Significantly different from DOX treatment.

Subfraction	MCF-7		MCF-7 ^{ADR}	
	IC ₅₀ (µg/ml)	R-fraction (%)	IC ₅₀ (µg/ml)	R-fraction (%)
B1	> 100	N/A	188.6 ± 2.3	N/A
B2	> 100	N/A	86.4 ± 1.5	N/A
B3	> 100	N/A	100.4 ± 1.8	N/A
B4	> 100	N/A	112.7 ± 2	N/A

Table 4. Cytotoxic effect of subfractions (B1–B4) of Fr-3 within MCF-7 and MCF7-^{ADR} cell lines. #N/A means not applicable.

Subfraction	MCF-7 ^{ADR}	
	(IC ₅₀ µg/mL)	R-fraction (%)
DOX	9.9 ± 1.1	5.2 ± 0.04
DOX + B1 (1:10)	1.5 ± 0.3*	N/A
CI index/ CI value	Synergism/0.157	
DOX + B2 (1:10)	0.03 ± 0.001*	N/A
CI index/ CI value	Synergism/0.003	
DOX + B3 (1:10)	0.35 ± 0.02*	N/A
CI index/ CI value	Synergism/0.038	
DOX + B4 (1:10)	0.56 ± 0.04*	N/A
CI index/ CI value	Synergism/0.061	

Table 5. Chemomodulatory effect of subfractions (B1–B4) of Fr-3 on the cytotoxicity of DOX against MCF-7^{ADR} cell line. #N/A means not applicable. Data are presented as mean ± SD; n = 3. *Significantly different from DOX treatment.

The effect of DOX, B2-fraction, and their combination on the intracellular GSH level within MCF-7^{ADR} cells. In this study, we tested the influence of the most potent cytotoxic fraction (B2) and doxorubicin alone or in combination on the intracellular level of GSH within MCF-7^{ADR} cells. Numerous studies have indicated GSH activity alterations after treatment with doxorubicin in vitro. Herein, it was found that DOX treatment resulted in a significant increase in GSH levels ($3.81 \pm 0.2 \mu\text{mol}/\text{mg}$ protein) compared to non-treated cells ($2.71 \pm 0.1 \mu\text{mol}/\text{mg}$ protein). On the other hand, B2 alone showed a significant reduction in GSH level to $1.67 \pm 0.5 \mu\text{mol}/\text{mg}$ protein compared to non-treated cells ($2.71 \pm 0.1 \mu\text{mol}/\text{mg}$ protein). The combination of B2-fraction and DOX normalized the intracellular GSH level and brought back to be non-significant from untreated cells (Fig. 4).

Discussion

RP-LC-DAD-ESI-QTOF-MS profiling of methanol extract and methylene chloride fraction. Untargeted metabolite profiling of the crude MeOH extract and the most active CH₂Cl₂ fraction with potential cytotoxicity was conducted using RP-LC-DAD-ESI-QTOF-MS. The results of the analysis revealed the identification of 53 in both extracts with different abundance using both ESI modes (Table 1). The metabolites were tentatively characterized based on their UV spectra (254, 280 and 330 nm), retention time, molecular weight, MS fragmentation patterns and comparing their mass spectra with those reported in the phytochemical dictionary of natural products database (CRC) and reported literature^{30–33}.

The identified metabolites (Fig. 3, Table 1) are belonging to different phytochemical classes, such as phenolic acids and phenolic derivatives (14), ellagitannins (12), flavonoids (10), fatty acids (7), lignans (6), and amino acid (1), sugar derivative (1), alkaloid (1), and dicarboxylic (1). Details of metabolites assignment will be discussed in the coming section.

Phenolic, phenolic acids, alkaloid, ellagitannins and flavonoid glycosides are eluted first in the chromatogram followed by fatty acids, flavonoid aglycones, while the lignans, and were emerged by end of the chromatogram. Most of peaks belonging to acids and phenolics compounds were observed in negative ion mode (Table 1).

Among the fifty-three identified metabolites, sixteen were reported in *P. niruri* for the first time and the metabolites identified were 1, 4, 5, 7, 8, 10, 30, 35, 36, 41–47. The rest of the metabolites are either previously identified in *P. niruri* or from other *Phyllanthus* species. The newly identified metabolites in *P. niruri* and in genus *Phyllanthus* are classified into sialic acid derivative (1), phenolics and phenolic acid derivatives (4, 7, 8, 10, and 30), organic acid (35), a flavonoid (36), polyketide alkaloid (5), and fatty acids (41–47).

Compound 1 was identified as 2-deoxy-2,3-dehydro-*N*-acetylneuraminic acid (sialic acid derivative) by observing mass ions at 290.0882 [M-H]⁻, and fragments at m/z 200.0567 [M-H-C₃H₆O₃]⁻, 128.0356 [M-H-C₃H₆O₃-C₃H₄O₂]⁻. This compound was previously identified in *Nymphaea nouchali* stem³⁴, and detected in edible bird's nest, a nutrient-rich salivary bioproduct produced by swiftlets in Southeast Asia³⁵.

Compound 4 was identified as vanillic acid 4-sulfate, previously isolated from seaweeds *Sargassum* sp., *Centroceras* sp., *Ulva* sp.³⁶, and detected in the urine of healthy rats supplemented for 35 days with cranberry extract³⁷. It showed a molecular ion peak [M-H]⁻ at m/z 290.0882, in addition to the fragmentation pattern with ions at m/z 203.0019 [M-H-CO₂]⁻, 121.0296 [M-H-CO₂-SH₂O₃]⁻, 108.0220 [M-H-CO₂-SH₂O₃-CH]⁻, 96.9604 [H₂SO₄]⁻, 80.9656 [H₂SO₃]⁻³⁸.

Compound 5 was identified as sesbanimide A based on the fragmentation pattern with ions at m/z 328.1399 [M+H]⁺, 310.1290 [M+H-H₂O]⁺, 250.1655 [M+H-H₂O-C₂H₄O₂]⁺, 232.1550 [M+H-2H₂O-C₂H₄O₂]⁺, 132.0811 [M+H-2H₂O-C₂H₄O₂-C₄H₄O₃]⁺, 120.0810 [M+H-2H₂O-C₂H₄O₂-C₅H₄O₃]⁺. This compound

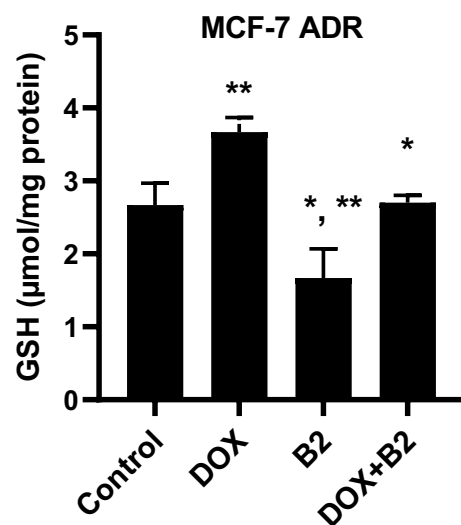


Figure 4. Effects of treatment with IC₅₀ values of B2-fraction, DOX alone or their combination on the intracellular level of GSH within MCF-7^{ADR} cells. Data are presented as mean ± SD; n = 3. *Significantly different from DOX treatment. **Significantly different from control.

was detected and isolated from two marine alphaproteobacteria *Stappia indica* PHM037 and *Labrenzia aggregata* PHM038³⁹, in Wu-Ling-San traditional Chinese formula⁴⁰, and from *Sesbania drummondii* seed⁴¹.

Compounds **7** and **8** had deprotonated molecular ions $[M-H]^-$ at m/z 371.0619 and 357.0826, and molecular formulae $C_{15}H_{16}O_{11}$ and $C_{15}H_{18}O_{10}$, respectively. They were tentatively identified as caffeoylglucaric acid isomer (**7**) isolated from edible wild calafate berry (*Berberis microphylla* G. Forst)⁴² and dihydrocaffeic acid 3-O-glucuronide (**8**) detected among the polyphenol-derived metabolites in human plasma after coffee consumption^{43–45}. The identification of compound **7** as caffeoylglucaric acid isomer was achieved through the presence of the fragment ions at m/z 315, 209 and 191. According the reported literature⁴², the fragment at m/z 209 can be interpreted as an aldaric acid moiety like glucaric, with subsequent loss of H_2O , to give rise the fragment ion at m/z 191 $[209 - H_2O]^-$. This compound was tentatively characterized to be caffeoylglucaric acid isomers, in agreement with the profiles previously reported for *B. microphylla* G. Forst and *B. thunbergii* DC⁴⁶. Compound **8** was tentatively identified as dihydrocaffeic acid 3-O-glucuronide with $[M-H]^-$ m/z at 357.0826, and further confirmed from ions at m/z 181 due to loss of glucuronide from parent ion⁴⁵.

P. niruri showed the presence of compound **10** for the first time, it showed a molecular ion peak $[M+H]^+$ at m/z 623.0883 corresponding the molecular formula $C_{26}H_{24}O_{18}$ with exact mass of 624.0963 and tentatively identified as dihydrovirganin. In addition, it showed the loss of $C_9H_8O_8$ fragment at m/z 355.0665 $[M-H-C_9H_8O_8]^-$, and 234.0405 $[M-H-C_9H_8O_8-C_7H_5O_2]^-$. The closely related virganin metabolite ($C_{26}H_{22}O_{18}$) was identified in *P. niruri*⁴⁷, *P. virgatus*⁴⁸, and in *P. urinaria* and *P. amarum*⁴⁹.

The metabolite **30** was tentatively characterized as elagitannin 4-O-brevifolincarboxyl- 1-O-galloyl-3,6-O-hexahydroxydiphenoyl-D-glucopyranose⁵⁰ with a molecular formula $C_{40}H_{28}O_{25}$ and exact mass of m/z 908.0920. It showed the presence of $[M-H]^-$ at m/z at 907.0847 and fragments of m/z at 611.0708, and 169.0141.

The metabolite **35** was tentatively identified as azelaic acid, a dicarboxylic acid had the molecular formula $C_9H_{16}O_4$ and exact mass of 18.0974. Azelaic acid produced m/z 187.0974 $[M-H]^-$ as the ion base peak in negative ion mode^{51,52}. Azelaic acid is an organic acid compound observed in wheat, rice, rye and barley and it has antimicrobial and anti-inflammatory properties, which make it effective in the treatment of skin conditions like acne and rosacea⁵¹.

Compound **36** was observed only in negative ion mode and was identified as 3,4,5,7-Tetrahydroxyflavone-8-sulfonic acid (luteolin-8-sulfonic acid), a flavone sulfonic acid had the molecular formula of $C_{15}H_{10}O_9S$ and exact mass of 366.0046 and m/z 364.9973 $[M-H]^-$. It showed mass ion m/z 285.0403 $[M-H-SO_3]^-$ corresponding to the loss of a sulfonyl group.

Peaks from **41** to **43** were identified as fatty acid isomers. They had deprotonated molecular ions $[M-H]^-$ at m/z 327.2175, and fragments ions at m/z 285.0797, 215.1289, 171.1027, 85.0299. They were identified as trihydroxy-octadecadienoic acid isomers. On the other hand, the peaks from **44** to **47** were identified as fatty acid isomers of trihydroxy-octadecanoic acid. They had deprotonated molecular ions $[M-H]^-$ at m/z 329.2332.

Six lignans were characterized in the current study, while only four were nirtetralin, phyllanthin, hypophyllanthin, and niranthin, were previously confirmed from our previous work²⁵.

Biological findings. Breast cancer continues to be a major global health problem and it possess high incidence rate in women with subsequent very high rates of morbidity and mortality^{53,54}. Doxorubicin (DOX) is one of the mostly used chemotherapeutic medications for breast cancer. While DOX treatment initially causes clinical responses, its longstanding success may be halted due to the emergence of drug toxicities and resistance⁵⁵. Currently, combining the natural products with chemotherapeutic agents has drawn researchers' attention as it was observed to enhance the effectiveness of conventional chemotherapeutic medications and/or safeguard patients from their adverse effects⁵⁶.

Therefore, in this study, we explored the potential cytotoxic activity of *P. niruri*, a well-established bioactive medicinal herb, as well as its potential influence on the cytotoxic profile of DOX in naive (MCF-7) and doxorubicin-resistant (MCF-7^{ADR}) breast cancer cells. The literature reported some in vivo and in vitro studies of anticancer activity of *P. niruri* in various types of malignancies⁵⁷. To the best of our knowledge, this is the initial investigation for the impact of *P. niruri* on resistant breast cancer cells.

According to our data, all tested extracts, and fractions of *P. niruri* till did not show any promising cytotoxicity against the breast cancer cells alone under investigation (MCF-7 & MCF-7^{ADR}) except for the methylene chloride fraction (F-3). It showed weak cytotoxicity against MCF-7 cells ($IC_{50} = 97.2 \mu g/ml$) and surprisingly higher activity against the DOX resistant breast cancer cells (MCF-7^{ADR}). These findings were consistent with a few previous reports for the potential anticancer activity of aqueous and methanolic extracts of *P. niruri* against MCF-7 cells^{20,58}.

However, the promising cytotoxicity of CH_2Cl_2 fraction against MCF-7^{ADR} cells may be in part due to the reported P-glycoprotein (Pgp) inhibitory activity of *Phyllanthus* extracts in Pgp overexpressing cell lines^{59,60}. The activity of Pgp is implicated in multidrug resistance (MDR) of breast cancer and MCF-7^{ADR} cell line is the commonly used breast cancer cell model for the study of MDR related resistance^{61,62}.

The discrepancy in the effectiveness of *P. niruri* different extracts against cancer cells may be attributed to the difference in the present of bioactive substances. Therefore, untargeted metabolite profiling of the MeOH extract and the active cytotoxic CH_2Cl_2 fraction was performed using LC-DAD-QToF. The LC-MS profiling of the active CH_2Cl_2 revealed the presence of main compounds such as the ellagitannin phyllanthussin U (observed in positive mode) and flavonoids galangin-8-sulfonic acid and niruriflavone (marked in negative ion mode), in addition to six lignans nirtetralin, phyllanthin, hypophyllanthin, niranthin and isolintetralin. These lignans are well known for their anticancer activities^{63,64} that enrich the active CH_2Cl_2 fraction as seen in LC-MS.

In MCF-7 cells, combining DOX with *P. niruri* extracts (except for CH_2Cl_2 fraction) at a sub-cytotoxic concentration unexpectedly resulted in an extensively negative modification of doxorubicin's activity. These

combinations not only didn't show improvement in DOX-induced viability inhibition but additionally showed an increase in the IC₅₀ values of DOX in combinations to nearly ten times of DOX alone, suggesting an antagonistic type of interaction. This makes a lot of sense if we consider the strong antioxidant properties (due to its phenolic content) of this fraction and the mode of action for DOX which involves the generation of reactive oxygen species. Also, this finding is in line with previous observations for the combinations that sometimes resulted in antagonistic effects suggesting that combination at different dose levels was diverse and specific to each combination and cell line⁶⁵. The involved mechanisms in these interactions between DOX and *P. niruri* warrants further evaluation.

Surprisingly, in MCF-7^{ADR}, the opposite occurred for most combinations with DOX, which showed potentiation of activity manifested by significant decrease in the IC₅₀ values of DOX in combinations. These findings suggested that *P. nurini* derivatives could be effective MDR reversal agents, and accordingly they will synergize the activity of most of the standard chemotherapeutics such as DOX⁶⁶. Another important observation, CH₂Cl₂ fraction showed the maximal DOX activity potentiation in both cell lines.

According to our observation, *P. nurini* CH₂Cl₂ fraction alone showed moderate anti-proliferative effects. However, it enhanced the cytotoxic profile of DOX by 4 folds and 40 folds against MCF-7 and MCF-7^{ADR}, respectively. Several studies described the significance of *Phyllanthus* alone as an anti-cancer agent against distinct types of malignancy^{20,22}. In addition, several publications including ours showed promising chemomodulatory activities of *Phyllanthus* to several chemotherapeutics in various types of malignancy^{65,67}.

Combining the results of the two cell lines, Fr-3 had the lowest IC₅₀ values against naïve and resistant MCF-7 cells. Thus, it was selected for further TLC fractionation and investigation for their cytotoxicity and chemomodulatory potential against breast cancer cells. In the same manner, subfractions behave, showing more cytotoxic activity as well as chemomodulatory effect against MCF-7^{ADR}. In addition, TLC fractionation showed that B2 subfraction (R_f 0.2–0.35) was the most potent one in terms of cytotoxicity when combined with DOX.

Some studies suggested that the production of reactive oxygen species (ROS) after DOX treatment is responsible for the cytotoxicity in cancer cells, which could stimulate the production of antioxidant enzymes, like GSH, as a protective defense mechanism of cancer cells making it resistant to oxidative damage. Similarly, greater sensitivity to DOX was observed in breast cancer when the GSH levels decreased^{68,69}. Herein, GSH level reduction observed by *Phyllanthus niruri* may explain the enhanced chemotherapeutic effect of DOX via sensitizing the resistant MCF-7^{ADR} cells⁷⁰.

This finding supports our hypothesis that combinations of plant extracts and chemotherapeutic agents may allow for a significant reduction in the dosage of the more toxic chemotherapeutic agent while retaining the therapeutic efficacy and minimizing toxicities not only in naïve tumor cells but also and to a greater extent in the resistant tumor cells. Therefore, additional studies are needed for separation of pure compounds and further elucidation of mechanistic studies for the anticancer and chemomodulatory effects in naïve as well as resistant breast cancer cells.

Conclusion

Combined pharmacotherapy is a common approach that would improve the anticancer activities of cytotoxic drugs while lowering chemo-resistance of cancer cells. Accordingly, and to the best of our knowledge, this is the first study considering anticancer properties of *P. niruri* in resistant breast cancer alone and in combination with DOX. *P. niruri* is a promising chemomodulatory agent against resistant breast cancer. Hence, future investigations should include its effect in detail on resistant breast cancer and other MDR overexpressing cancer cells.

Data availability

All data generated or analyzed during this study are included in this published article and its supplementary information file.

Received: 22 July 2022; Accepted: 7 February 2023

Published online: 15 February 2023

References

- Fontana, F., Anselmi, M. & Limonta, P. Molecular mechanisms of cancer drug resistance: emerging biomarkers and promising targets to overcome tumor progression. *Cancers (Basel)* <https://doi.org/10.3390/cancers14071614> (2022).
- Ben Toumia, I. *et al.* A methanol extract of *Scabiosa atropurpurea* enhances doxorubicin cytotoxicity against resistant colorectal cancer cells in vitro. *Molecules* <https://doi.org/10.3390/molecules25225265> (2020).
- Khasraw, M., Bell, R. & Dang, C. Epirubicin: is it like doxorubicin in breast cancer? A clinical review. *Breast* **21**, 142–149 (2012).
- Łukasiewicz, S. *et al.* Breast cancer—epidemiology, risk factors, classification, prognostic markers, and current treatment strategies: an updated review. *Cancers* **13**, 4287 (2021).
- Liu, Y., Wang, M., Liu, W., Jing, J. & Ma, H. Olaparib and doxorubicin co-loaded polypeptide Nanogel for enhanced breast cancer therapy. *Front Bioeng Biotechnol* **10**, 904344. <https://doi.org/10.3389/fbioe.2022.904344> (2022).
- Argenziano, M. *et al.* Improvement in the anti-tumor efficacy of doxorubicin nanosponges in in vitro and in mice bearing breast tumor models. *Cancers Basel* <https://doi.org/10.3390/cancers12010162> (2020).
- Ibrahim-Fouad, G. & Ahmed, K. A. Curcumin ameliorates doxorubicin-induced cardiotoxicity and hepatotoxicity via suppressing oxidative stress and modulating iNOS, NF-κB, and TNF-α in rats. *Cardiovasc Toxicol.* **22**, 152–166 (2022).
- Okpara, E. S. *et al.* Molecular mechanisms associated with the chemoprotective role of protocatechuic acid and its potential benefits in the amelioration of doxorubicin-induced cardiotoxicity: a review. *Toxicol. Rep.* (2022).
- Hadi, N. A., Mahmood, R. I. & Al-Saffar, A. Z. Evaluation of antioxidant enzyme activity in doxorubicin treated breast cancer patients in Iraq: a molecular and cytotoxic study. *Gene Rep.* **24**, 101285 (2021).
- Cheraghi, O. *et al.* The effect of Nrf2 deletion on the proteomic signature in a human colorectal cancer cell line. *BMC Cancer* **22**, 1–16 (2022).

11. Henidi, H. A., Al-Abbasi, F. A., El-Moselhy, M. A., El-Bassossy, H. M. & Al-Abd, A. M. Despite blocking doxorubicin-induced vascular damage, quercetin ameliorates its antibreast cancer activity. *Oxid Med Cell Longev* **2020**, 8157640. <https://doi.org/10.1155/2020/8157640> (2020).
12. Shrihastini, V. *et al.* Plant derived bioactive compounds, their anti-cancer effects and in silico approaches as an alternative target treatment strategy for breast cancer: an updated overview. *Cancers Basel* <https://doi.org/10.3390/cancers13246222> (2021).
13. Nisar, M. F. *et al.* Chemical components and biological activities of the genus *Phyllanthus*: a review of the recent literature. *Molecules* <https://doi.org/10.3390/molecules23102567> (2018).
14. Manjrekar, A. P. *et al.* Effect of *Phyllanthus niruri* Linn. treatment on liver, kidney and testes in CCl₄ induced hepatotoxic rats. *Indian J Exp Biol* **46**, 514–520 (2008).
15. Najari Beidokhti, M. *et al.* Investigation of antidiabetic potential of *Phyllanthus niruri* L. using assays for alpha-glucosidase, muscle glucose transport, liver glucose production, and adipogenesis. *Biochem Biophys Res Commun* **493**, 869–874. <https://doi.org/10.1016/j.bbrc.2017.09.080> (2017).
16. Al Zarzour, R. H. *et al.* *Phyllanthus niruri* standardized extract alleviates the progression of non-alcoholic fatty liver disease and decreases atherosclerotic risk in sprague-dawley rats. *Nutrients* **9**, 55. <https://doi.org/10.3390/nu9070766> (2017).
17. Marhaeny, H. D., Widyawaruyanti, A., Widiandani, T., Fuad Hafid, A. & Wahyuni, T. S. *Phyllanthin* and *hypophyllanthin*, the isolated compounds of *Phyllanthus niruri* inhibit protein receptor of corona virus (COVID-19) through in silico approach. *J Basic Clin Physiol Pharmacol* **32**, 809–815. <https://doi.org/10.1515/jbcp-2020-0473> (2021).
18. Paul, S., Patra, D. & Kundu, R. Lignan enriched fraction (LRF) of *Phyllanthus amarus* promotes apoptotic cell death in human cervical cancer cells in vitro. *Sci Rep* **9**, 14950. <https://doi.org/10.1038/s41598-019-51480-7> (2019).
19. Young, A. N. *et al.* *Phyllanthus*min derivatives induce apoptosis and reduce tumor burden in high-grade serous ovarian cancer by late-stage autophagy inhibition. *Mol Cancer Ther* **17**, 2123–2135. <https://doi.org/10.1158/1535-5362.310528> (2018).
20. Lee, S. H., Jaganath, I. B., Wang, S. M. & Sekaran, S. D. Antimetastatic effects of *Phyllanthus* on human lung (A549) and breast (MCF-7) cancer cell lines. *PLoS ONE* **6**, e20994. <https://doi.org/10.1371/journal.pone.0020994> (2011).
21. Ramadhani, A. H. *et al.* Suppression of hypoxia and inflammatory pathways by *Phyllanthus niruri* extract inhibits angiogenesis in DMBA-induced breast cancer mice. *Res Pharm Sci* **16**, 217–226. <https://doi.org/10.1155/2021/4514342> (2021).
22. Tang, Y. Q., Jaganath, I., Manikam, R. & Sekaran, S. D. *Phyllanthus* suppresses prostate cancer cell, PC-3, proliferation and induces apoptosis through multiple signalling pathways (MAPKs, PI3K/Akt, NFkappaB, and hypoxia). *Evid Based Complement Alternat Med* **609**, 55. <https://doi.org/10.1155/2013/609581> (2013).
23. de Araujo Junior, R. F. *et al.* A dry extract of *Phyllanthus niruri* protects normal cells and induces apoptosis in human liver carcinoma cells. *Exp Biol Med Maywood* **237**, 1281–1288. <https://doi.org/10.1258/ebm.2012.012130> (2012).
24. Saahene, R. O. *et al.* A review: mechanism of *Phyllanthus urinaria* in cancers-NF-kappaB, PI3K/AKT, and MAPKs signaling activation. *Evid Based Complement Alternat Med* **2021**, 4514342. <https://doi.org/10.1155/2021/4514342> (2021).
25. Meselhy, M. R. *et al.* Preparation of Lignan-rich extract from the aerial parts of *Phyllanthus niruri* using nonconventional methods. *Molecules* **25**, 1179 (2020).
26. Skehan, P. *et al.* New colorimetric cytotoxicity assay for anticancer-drug screening. *JNCI: J. Natl. Cancer Inst.* **82**, 1107–1112 (1990).
27. Eldeeb, M. *et al.* Anticancer effects with molecular docking confirmation of newly synthesized Isatin sulfonamide molecular hybrid derivatives against hepatic cancer cell lines. *Biomedicines* **10**, 722 (2022).
28. Allam, R. M. *et al.* Fingolimod interrupts the cross talk between estrogen metabolism and sphingolipid metabolism within prostate cancer cells. *Toxicol Lett* **291**, 77–85. <https://doi.org/10.1016/j.toxlet.2018.04.008> (2018).
29. Chou, T. C. & Talalay, P. Quantitative analysis of dose-effect relationships: the combined effects of multiple drugs or enzyme inhibitors. *Adv Enzyme Regul* **22**, 27–55. [https://doi.org/10.1016/0065-2571\(84\)90007-4](https://doi.org/10.1016/0065-2571(84)90007-4) (1984).
30. Buckingham, J. *Dictionary of natural products*. (CRC Press, 1993).
31. Kumar, B., Kumar, S. & Madhusudanan, K. *Phytochemistry of Plants of Genus Phyllanthus*. (CRC Press, 2020).
32. Kumar, S., Singh, A. & Kumar, B. Identification and characterization of phenolics and terpenoids from ethanolic extracts of *Phyllanthus* species by HPLC-ESI-QTOF-MS/MS. *J. Pharmaceutical Anal.* **7**, 214–222 (2017).
33. Yang, B., Kortensniemi, M., Liu, P., Karonen, M. & Salminen, J.-P. Analysis of hydrolyzable tannins and other phenolic compounds in emblic leafflower (*Phyllanthus emblica* L.) fruits by high performance liquid chromatography–electrospray ionization mass spectrometry. *J. Agric. Food Chem.* **60**, 8672–8683 (2012).
34. Alam, M. B. *et al.* High resolution mass spectroscopy-based secondary metabolite profiling of *Nymphaea nouchali* (Burm. f) stem attenuates oxidative stress via regulation of MAPK/Nrf2/HO-1/ROS pathway. *Antioxidants* **10**, 719 (2021).
35. Tong, S.-R., Lee, T.-H., Cheong, S.-K. & Lim, Y.-M. Untargeted metabolite profiling on the water-soluble metabolites of edible bird's nest through liquid chromatography-mass spectrometry. *Veterinary World* **13**, 304 (2020).
36. Zhong, B. *et al.* Lc-esi-qtof-ms/ms characterization of seaweed phenolics and their antioxidant potential. *Mar. Drugs* **18**, 331 (2020).
37. Peron, G. *et al.* Antiadhesive activity and metabolomics analysis of rat urine after cranberry (*Vaccinium macrocarpon* Aiton) administration. *J. Agric. Food Chem.* **65**, 5657–5667 (2017).
38. Correia, M. S., Ballet, C., Meistermann, H., Conway, L. P. & Globisch, D. Comprehensive kinetic and substrate specificity analysis of an arylsulfatase from *Helix pomatia* using mass spectrometry. *Bioorg. Med. Chem.* **27**, 955–962 (2019).
39. Kacar, D. *et al.* Identification of trans-AT polyketide clusters in two marine bacteria reveals cryptic similarities between distinct symbiosis factors. *Environ. Microbiol.* **23**, 2509–2521 (2021).
40. Xiao, S. *et al.* Deciphering the differentiations of traditional Chinese medicine analogous formulae by parallel liquid chromatography-mass spectrometry coupled with microplate-based assays. *Anal. Methods* **6**, 9283–9290 (2014).
41. Powell, R. G., Smith, C. R. Jr. & Weisleder, D. Sesbanimide A and related tumor inhibitors from *Sesbania drummondii*: structure and chemistry. *Phytochemistry* **23**, 2789–2796 (1984).
42. Ruiz, A. *et al.* Isolation and structural elucidation of anthocyanidin 3, 7-β-O-diglucosides and caffeoyl-glucuronic acids from calafate berries. *J. Agric. Food Chem.* **62**, 6918–6925 (2014).
43. Redeuil, K. *et al.* Identification of novel circulating coffee metabolites in human plasma by liquid chromatography–mass spectrometry. *J. Chromatogr. A* **1218**, 4678–4688 (2011).
44. Farrell, T., Poquet, L., Dionisi, F., Barron, D. & Williamson, G. Characterization of hydroxycinnamic acid glucuronide and sulfate conjugates by HPLC–DAD–MS2: enhancing chromatographic quantification and application in Caco-2 cell metabolism. *J. Pharm. Biomed. Anal.* **55**, 1245–1254 (2011).
45. Sasot, G. *et al.* Identification of phenolic metabolites in human urine after the intake of a functional food made from grape extract by a high resolution LTQ-Orbitrap-MS approach. *Food Res. Int.* **100**, 435–444 (2017).
46. Fernández-Poyatos, M. D. P., Ruiz-Medina, A., Zengin, G. & Llorent-Martínez, E. J. Phenolic characterization, antioxidant activity, and enzyme inhibitory properties of *Berberis thunbergii* DC. leaves: a valuable source of phenolic acids. *Molecules* **24**, 4171 (2019).
47. Sousa, A. *et al.* UPLC-QTOF-MSE-based chemometric approach driving the choice of the best extraction process for *Phyllanthus niruri*. *Sep. Sci. Technol.* **52**, 1696–1706 (2017).
48. Huang, Y.-L., Chen, C.-C., Hsu, F.-L. & Chen, C.-F. Tannins, flavonol sulfonates, and a Norlignan from *Phyllanthus virgatus*. *J. Nat. Prod.* **61**, 1194–1197 (1998).
49. Guo, J. *et al.* Comparison of two exploratory data analysis methods for classification of *Phyllanthus* chemical fingerprint: unsupervised vs. supervised pattern recognition technologies. *Anal. Bioanal. Chem.* **407**, 1389–1401 (2015).

50. da Fontoura Sprenger, R. & Cass, Q. B. Characterization of four *Phyllanthus* species using liquid chromatography coupled to tandem mass spectrometry. *J. Chromatography A* **1291**, 97–103 (2013).
51. de Almeida, R. T. R. *et al.* Exploring the rumen fluid metabolome using liquid chromatography-high-resolution mass spectrometry and Molecular Networking. *Sci. Rep.* **8**, 1–8 (2018).
52. Romero, N. *et al.* In vitro anthelmintic evaluation of *Gliricidia sepium*, *Leucaena leucocephala*, and *Pithecellobium dulce*: fingerprint analysis of extracts by UHPLC-orbitrap mass spectrometry. *Molecules* **25**, 3002 (2020).
53. Barrios, C. H. Global challenges in breast cancer detection and treatment. *Breast* **62**(Suppl 1), S3–S6. <https://doi.org/10.1016/j.breast.2022.02.003> (2022).
54. Mahmood, R. I., Abbas, A. K., Razali, N., Al-Saffar, A. Z. & Al-Obaidi, J. R. Protein profile of MCF-7 breast cancer cell line treated with lectin delivered by CaCO₃NPs revealed changes in molecular chaperones, cytoskeleton, and membrane-associated proteins. *Int. J. Biol. Macromol.* **184**, 636–647 (2021).
55. Howard, G. R., Jost, T. A., Yankeelov, T. E. & Brock, A. Quantification of long-term doxorubicin response dynamics in breast cancer cell lines to direct treatment schedules. *PLoS Comput Biol* **18**, e1009104, doi:<https://doi.org/10.1371/journal.pcbi.1009104> (2022).
56. Ali Abdalla, Y. O. *et al.* Natural products for cancer therapy: a review of their mechanism of actions and toxicity in the past decade. *J Trop Med* **2022**, 5794350. <https://doi.org/10.1155/2022/5794350> (2022).
57. Kalimuthu, A. K. *et al.* In silico, in vitro screening of antioxidant and anticancer potentials of bioactive secondary metabolites from an endophytic fungus (*Curvularia* sp.) from *Phyllanthus niruri* L. *Environ Sci Pollut Res Int*, doi:<https://doi.org/10.1007/s11356-022-19249-0> (2022).
58. Lee, S. H., Jaganath, I. B., Atiya, N., Manikam, R. & Sekaran, S. D. Suppression of ERK1/2 and hypoxia pathways by four *Phyllanthus* species inhibits metastasis of human breast cancer cells. *J Food Drug Anal* **24**, 855–865. <https://doi.org/10.1016/j.jfda.2016.03.010> (2016).
59. Patel, J. R., Tripathi, P., Sharma, V., Chauhan, N. S. & Dixit, V. K. *Phyllanthus amarus*: ethnomedicinal uses, phytochemistry and pharmacology: a review. *J Ethnopharmacol* **138**, 286–313. <https://doi.org/10.1016/j.jep.2011.09.040> (2011).
60. Kassuya, C. A., Leite, D. F., de Melo, L. V., Rehder, V. L. & Calixto, J. B. Anti-inflammatory properties of extracts, fractions and lignans isolated from *Phyllanthus amarus*. *Planta Med* **71**, 721–726. <https://doi.org/10.1055/s-2005-871258> (2005).
61. Chen, C. H. *et al.* Overcoming multidrug resistance of breast cancer cells by the micellar doxorubicin nanoparticles of mPEG-PCL-graft-cellulose. *J Nanosci Nanotechnol* **11**, 53–60. <https://doi.org/10.1166/jnn.2011.3102> (2011).
62. Howard, G. R., Johnson, K. E., Rodriguez Ayala, A., Yankeelov, T. E. & Brock, A. A multi-state model of chemoresistance to characterize phenotypic dynamics in breast cancer. *Sci Rep* **8**, 12058. <https://doi.org/10.1038/s41598-018-30467-w> (2018).
63. Ooi, K. L., Loh, S. I., Sattar, M. A., Muhammad, T. S. T. & Sulaiman, S. F. Cytotoxic, caspase-3 induction and in vivo hepatoprotective effects of phyllanthin, a major constituent of *Phyllanthus niruri*. *J. Funct. Foods* **14**, 236–243 (2015).
64. Sujatha, R., Norhanom, A. W., Nurhayati, Z. A. & Sugumaran, M. Cytotoxicity evaluation of five selected Malaysian *Phyllanthaceae* species on various human cancer cell lines. *Journal of Medicinal Plants Research* **5**, 2267–2273 (2011).
65. Pinmai, K., Chunlaratthanabhorn, S., Ngamkitidechakul, C., Soonthornchareon, N. & Hahnvajjanawong, C. Synergistic growth inhibitory effects of *Phyllanthus emblica* and *Terminalia bellerica* extracts with conventional cytotoxic agents: doxorubicin and cisplatin against human hepatocellular carcinoma and lung cancer cells. *World J Gastroenterol* **14**, 1491–1497. <https://doi.org/10.3748/wjg.14.1491> (2008).
66. Leite, D. F. *et al.* The cytotoxic effect and the multidrug resistance reversing action of lignans from *Phyllanthus amarus*. *Planta Med* **72**, 1353–1358. <https://doi.org/10.1055/s-2006-951708> (2006).
67. Guo, J. R. *et al.* Effect of *Phyllanthus amarus* extract on 5-fluorouracil-induced perturbations in ribonucleotide and deoxyribonucleotide pools in HepG2 cell line. *Molecules* **21**, doi:<https://doi.org/10.3390/molecules21091254> (2016).
68. Leonel, C. *et al.* Expression of glutathione, glutathione peroxidase and glutathione S-transferase pi in canine mammary tumors. *BMC Vet. Res.* **10**, 1–10 (2014).
69. Salama, M. M., Zaghoul, R. A., Khalil, R. M. & El-Shishtawy, M. M. Sitagliptin potentiates the anti-neoplastic activity of doxorubicin in experimentally-induced mammary adenocarcinoma in mice: implication of oxidative stress, inflammation, angiogenesis, and apoptosis. *Sci. Pharm.* **90**, 42 (2022).
70. Prasad, N. R., Muthusamy, G., Shanmugam, M. & Ambudkar, S. V. South Asian medicinal compounds as modulators of resistance to chemotherapy and radiotherapy. *Cancers* **8**, 32 (2016).

Acknowledgements

This research was made possible as part of the Ministry of Agriculture Malaysia initiative under the New Key Economic Areas Entry Point Project on High Value Herbals awarded to Natural Wellness Biotech (M) Sdn Bhd. The authors express their gratitude and appreciation for the trust and opportunity given.

Author contributions

O.E.A.: Methodology, Investigation, Data curation. R.M.A.: Conceptualization, Supervision, Methodology, Investigation, Writing-Original draft preparation, Writing-Reviewing, and Editing. A.M.A.: Conceptualization, Writing-Original draft preparation, Writing-Reviewing, and Editing. A.E.: Conceptualization, Supervision, Methodology, Validation, Investigation, Writing-Original draft preparation, Writing-Reviewing, and Editing. B.A.: Conceptualization, Methodology, Data Analysis, Writing-Original draft preparation, Writing-Reviewing, and Editing. K.K.: Methodology, Investigation, Data Analysis, Writing-Reviewing, and Editing. I.A.K.: Conceptualization, Visualization, Writing-Reviewing, and Editing. E.A.: Conceptualization, Original draft preparation, Writing-Reviewing, and Editing. M.R.M.: Conceptualization, Supervision, Original draft preparation, Writing-Reviewing and Editing. A.M.E.: Conceptualization and Writing-Reviewing and Editing. S.O.M.: Conceptualization, Supplying plant material, Editing.

Funding

Open access funding provided by The Science, Technology & Innovation Funding Authority (STDF) in cooperation with The Egyptian Knowledge Bank (EKB).

Competing interests

The authors declare that they have no competing interests.

Additional information

Supplementary Information The online version contains supplementary material available at <https://doi.org/10.1038/s41598-023-29566-0>.

Correspondence and requests for materials should be addressed to E.A.-S.

Reprints and permissions information is available at www.nature.com/reprints.

Publisher's note Springer Nature remains neutral with regard to jurisdictional claims in published maps and institutional affiliations.



Open Access This article is licensed under a Creative Commons Attribution 4.0 International License, which permits use, sharing, adaptation, distribution and reproduction in any medium or format, as long as you give appropriate credit to the original author(s) and the source, provide a link to the Creative Commons licence, and indicate if changes were made. The images or other third party material in this article are included in the article's Creative Commons licence, unless indicated otherwise in a credit line to the material. If material is not included in the article's Creative Commons licence and your intended use is not permitted by statutory regulation or exceeds the permitted use, you will need to obtain permission directly from the copyright holder. To view a copy of this licence, visit <http://creativecommons.org/licenses/by/4.0/>.

© The Author(s) 2023